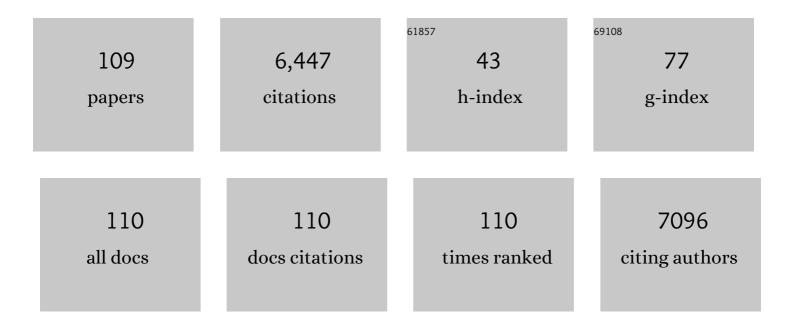
## List of Publications by Year in descending order

Source: https://exaly.com/author-pdf/1047703/publications.pdf Version: 2024-02-01



#	Article	IF	CITATIONS
1	A three-dimensional porous LiFePO <sub>4</sub> cathode material modified with a nitrogen-doped graphene aerogel for high-power lithium ion batteries. Energy and Environmental Science, 2015, 8, 869-875.	15.6	412
2	Graphene-based composites for electrochemical energy storage. Energy Storage Materials, 2020, 24, 22-51.	9.5	364
3	Nitrogenâ€Doped Graphene Ribbon Assembled Core–Sheath MnO@Graphene Scrolls as Hierarchically Ordered 3D Porous Electrodes for Fast and Durable Lithium Storage. Advanced Functional Materials, 2016, 26, 7754-7765.	7.8	245
4	Anodic Oxidation Strategy toward Structure-Optimized V <sub>2</sub> O <sub>3</sub> Cathode <i>via</i> Electrolyte Regulation for Zn-Ion Storage. ACS Nano, 2020, 14, 7328-7337.	7.3	229
5	A Hierarchical Porous C@LiFePO <sub>4</sub> /Carbon Nanotubes Microsphere Composite for Highâ€Rate Lithiumâ€Ion Batteries: Combined Experimental and Theoretical Study. Advanced Energy Materials, 2016, 6, 1600426.	10.2	194
6	Flexible Transparent Molybdenum Trioxide Nanopaper for Energy Storage. Advanced Materials, 2016, 28, 6353-6358.	11.1	194
7	Prelithiation: A Crucial Strategy for Boosting the Practical Application of Next-Generation Lithium Ion Battery. ACS Nano, 2021, 15, 2197-2218.	7.3	192
8	Vertically Aligned Sulfur–Graphene Nanowalls on Substrates for Ultrafast Lithium–Sulfur Batteries. Nano Letters, 2015, 15, 3073-3079.	4.5	183
9	Synergistic deficiency and heterojunction engineering boosted VO2 redox kinetics for aqueous zinc-ion batteries with superior comprehensive performance. Energy Storage Materials, 2020, 33, 390-398.	9.5	178
10	Solid Electrolyte Interphases on Sodium Metal Anodes. Advanced Functional Materials, 2020, 30, 2004891.	7.8	154
11	Effective Chemical Prelithiation Strategy for Building a Silicon/Sulfur Li-Ion Battery. ACS Energy Letters, 2019, 4, 1717-1724.	8.8	151
12	3D self-supported hierarchical core/shell structured MnCo <sub>2</sub> O <sub>4</sub> @CoS arrays for high-energy supercapacitors. Journal of Materials Chemistry A, 2018, 6, 1822-1831.	5.2	141
13	Mesoporous carbon-coated LiFePO <sub>4</sub> nanocrystals co-modified with graphene and Mg <sup>2+</sup> doping as superior cathode materials for lithium ion batteries. Nanoscale, 2014, 6, 986-995.	2.8	139
14	Hierarchical design of hollow Co-Ni LDH nanocages strung by MnO2 nanowire with enhanced pseudocapacitive properties. Energy Storage Materials, 2019, 19, 370-378.	9.5	127
15	LiFePO4 quantum-dots composite synthesized by a general microreactor strategy for ultra-high-rate lithium ion batteries. Nano Energy, 2017, 42, 363-372.	8.2	121
16	Construction of Structure-Tunable Si@Void@C Anode Materials for Lithium-Ion Batteries through Controlling the Growth Kinetics of Resin. ACS Nano, 2019, 13, 12219-12229.	7.3	119
17	Electrodeposition: Synthesis of advanced transition metal-based catalyst for hydrogen production via electrolysis of water. Journal of Energy Chemistry, 2021, 57, 547-566.	7.1	116
18	From Commercial Sponge Toward 3D Graphene–Silicon Networks for Superior Lithium Storage. Advanced Energy Materials, 2015, 5, 1500289.	10.2	114

#	Article	IF	CITATIONS
19	In situ one-step synthesis of CoFe2O4/graphene nanocomposites as high-performance anode for lithium-ion batteries. Electrochimica Acta, 2014, 129, 33-39.	2.6	113
20	Synergistic nanostructure and heterointerface design propelled ultra-efficient in-situ self-transformation of zinc-ion battery cathodes with favorable kinetics. Nano Energy, 2021, 81, 105601.	8.2	113
21	Desired crystal oriented LiFePO <sub>4</sub> nanoplatelets in situ anchored on a graphene cross-linked conductive network for fast lithium storage. Nanoscale, 2015, 7, 8819-8828.	2.8	107
22	Graphene-reinforced aluminum matrix composites prepared by spark plasma sintering. International Journal of Minerals, Metallurgy and Materials, 2016, 23, 723-729.	2.4	106
23	Improvement of the electrochemical performance of carbon-coated LiFePO <sub>4</sub> modified with reduced graphene oxide. Journal of Materials Chemistry A, 2013, 1, 135-144.	5.2	104
24	Interfacial and Electronic Modulation via Localized Sulfurization for Boosting Lithium Storage Kinetics. Advanced Materials, 2020, 32, e2000151.	11.1	98
25	NiCo <sub>2</sub> S <sub>4</sub> nanotube arrays grown on flexible nitrogen-doped carbon foams as three-dimensional binder-free integrated anodes for high-performance lithium-ion batteries. Physical Chemistry Chemical Physics, 2016, 18, 4505-4512.	1.3	90
26	Preparation of nickel nanoparticle/graphene composites for non-enzymatic electrochemical glucose biosensor applications. Materials Research Bulletin, 2014, 49, 521-524.	2.7	85
27	Hierarchical NiMoO <sub>4</sub> nanowire arrays supported on macroporous graphene foam as binder-free 3D anodes for high-performance lithium storage. Physical Chemistry Chemical Physics, 2016, 18, 908-915.	1.3	82
28	All-climate sodium ion batteries based on the NASICON electrode materials. Nano Energy, 2016, 30, 756-761.	8.2	81
29	Pitting corrosion of naturally aged AA 7075 aluminum alloys with bimodal grain size. Corrosion Science, 2016, 113, 1-16.	3.0	77
30	Modified solid-electrolyte interphase toward stable Li metal anode. Nano Energy, 2020, 77, 105308.	8.2	75
31	Integration of network-like porous NiMoO <sub>4</sub> nanoarchitectures assembled with ultrathin mesoporous nanosheets on three-dimensional graphene foam for highly reversible lithium storage. Journal of Materials Chemistry A, 2015, 3, 13691-13698.	5.2	72
32	Biomass chitin-derived honeycomb-like nitrogen-doped carbon/graphene nanosheet networks for applications in efficient oxygen reduction and robust lithium storage. Journal of Materials Chemistry A, 2016, 4, 11789-11799.	5.2	71
33	A 3D conductive scaffold with lithiophilic modification for stable lithium metal batteries. Journal of Materials Chemistry A, 2018, 6, 17967-17976.	5.2	57
34	The composite electrode of LiFePO <sub>4</sub> cathode materials modified with exfoliated graphene from expanded graphite for high power Li-ion batteries. Journal of Materials Chemistry A, 2014, 2, 2822-2829.	5.2	51
35	Carbon nanotube decorated NaTi <sub>2</sub> (PO <sub>4</sub> ) <sub>3</sub> /C nanocomposite for a high-rate and low-temperature sodium-ion battery anode. RSC Advances, 2016, 6, 70277-70283.	1.7	51
36	Self-assembly of ultrathin mesoporous CoMoO <sub>4</sub> nanosheet networks on flexible carbon fabric as a binder-free anode for lithium-ion batteries. New Journal of Chemistry, 2016, 40, 2259-2267.	1.4	51

BO WANG

#	Article	IF	CITATIONS
37	From biomass chitin to mesoporous nanosheets assembled loofa sponge-like N-doped carbon/g-C 3 N 4 3D network architectures as ultralow-cost bifunctional oxygen catalysts. Microporous and Mesoporous Materials, 2017, 240, 216-226.	2.2	51
38	Hierarchical heterostructures of NiO nanosheet arrays grown on pine twig-like β-NiS@Ni3S2 frameworks as free-standing integrated anode for high-performance lithium-ion batteries. Chemical Engineering Journal, 2019, 356, 245-254.	6.6	51
39	Holey graphene modified LiFePO4 hollow microsphere as an efficient binary sulfur host for high-performance lithium-sulfur batteries. Energy Storage Materials, 2020, 26, 433-442.	9.5	49
40	An efficient route to a hierarchical CoFe 2 O 4 @graphene hybrid films with superior cycling stability and rate capability for lithium storage. Electrochimica Acta, 2014, 146, 679-687.	2.6	48
41	In situ template synthesis of hollow nanospheres assembled from NiCo <sub>2</sub> S <sub>4</sub> @C ultrathin nanosheets with high electrochemical activities for lithium storage and ORR catalysis. Physical Chemistry Chemical Physics, 2017, 19, 11554-11562.	1.3	47
42	The synergy effect on Li storage of LiFePO4 with activated carbon modifications. RSC Advances, 2013, 3, 20024.	1.7	46
43	A MIL-47(V) derived hierarchical lasagna-structured V <sub>2</sub> O <sub>3</sub> @C hollow microcuboid as an efficient sulfur host for high-performance lithium–sulfur batteries. Nanoscale, 2020, 12, 4552-4561.	2.8	44
44	Boosting electrochemical kinetics of S cathodes for room temperature Na/S batteries. Matter, 2021, 4, 1768-1800.	5.0	39
45	In situ growth of CuO submicro-sheets on optimized Cu foam to induce uniform Li deposition and stripping for stable Li metal batteries. Electrochimica Acta, 2020, 339, 135941.	2.6	36
46	Improving weld strength of arc-assisted ultrasonic seam welded Mg/Al joint with Sn interlayer. Materials and Design, 2016, 98, 262-271.	3.3	35
47	Core-shell structured Fe 3 O 4 @NiS nanocomposite as high-performance anode material for alkaline nickel-iron rechargeable batteries. Electrochimica Acta, 2017, 231, 479-486.	2.6	35
48	Free-standing 3D network-like cathode based on biomass-derived N-doped carbon/graphene/g-C3N4 hybrid ultrathin sheets as sulfur host for high-rate Li-S battery. Renewable Energy, 2020, 158, 509-519.	4.3	34
49	Iron selenide nanoparticles-encapsulated within bamboo-like N-doped carbon nanotubes as composite anodes for superior lithium and sodium-ion storage. Chemical Engineering Journal, 2022, 435, 135185.	6.6	33
50	A new reflowing strategy based on lithiophilic substrates towards smooth and stable lithium metal anodes. Journal of Materials Chemistry A, 2019, 7, 18126-18134.	5.2	32
51	Trifunctional Electrode Additive for High Active Material Content and Volumetric Lithiumâ€lon Electrode Densities. Advanced Energy Materials, 2019, 9, 1803390.	10.2	32
52	Growth of LiFePO4 nanoplatelets with orientated (010) facets on graphene for fast lithium storage. Materials Letters, 2014, 118, 137-141.	1.3	31
53	Carbon-coated single-crystalline LiFePO4 nanocomposites for high-power Li-ion batteries: the impact of minimization of the precursor particle size. RSC Advances, 2014, 4, 10067.	1.7	31
54	Electrophoretic deposition of hierarchical Co <sub>3</sub> O <sub>4</sub> @graphene hybrid films as binder-free anodes for high-performance lithium-ion batteries. RSC Advances, 2015, 5, 33438-33444.	1.7	31

#	Article	IF	CITATIONS
55	Metal–organic framework derived amorphous VO <sub>x</sub> coated Fe <sub>3</sub> O <sub>4</sub> /C hierarchical nanospindle as anode material for superior lithium-ion batteries. Nanoscale, 2020, 12, 16901-16909.	2.8	31
56	Sodiophilic Decoration of a Three-Dimensional Conductive Scaffold toward a Stable Na Metal Anode. ACS Sustainable Chemistry and Engineering, 2020, 8, 5452-5463.	3.2	31
57	A novel 3D POMOF based on Wells–Dawson arsenomolybdates with excellent photocatalytic and lithium-ion battery performance. CrystEngComm, 2017, 19, 7154-7161.	1.3	30
58	Modifying hydrogel electrolyte to induce zinc deposition for dendrite-free zinc metal anode. Electrochimica Acta, 2021, 393, 139094.	2.6	30
59	Suppressing lithium dendrites within inorganic solid-state electrolytes. Cell Reports Physical Science, 2022, 3, 100706.	2.8	30
60	Facile and large-scale fabrication of hierarchical ZnFe <sub>2</sub> O <sub>4</sub> /graphene hybrid films as advanced binder-free anodes for lithium-ion batteries. New Journal of Chemistry, 2015, 39, 1725-1733.	1.4	29
61	Self-assembly of 2D sandwich-structured MnFe2O4/graphene composites for high-performance lithium storage. Materials Research Bulletin, 2015, 61, 369-374.	2.7	29
62	Nanocrystal-constructed mesoporous CoFe <sub>2</sub> O <sub>4</sub> nanowire arrays aligned on flexible carbon fabric as integrated anodes with enhanced lithium storage properties. Physical Chemistry Chemical Physics, 2015, 17, 21476-21484.	1.3	28
63	N-doped graphene/Bi nanocomposite with excellent electrochemical properties for lithium–ion batteries. Ionics, 2017, 23, 1407-1415.	1.2	28
64	Synergistic Interfacial and Doping Engineering of Heterostructured NiCo(OH)x-CoyW as an Efficient Alkaline Hydrogen Evolution Electrocatalyst. Nano-Micro Letters, 2021, 13, 120.	14.4	28
65	MoO2 nanobelts modified with an MOF-derived carbon layer for high performance lithium-ion battery anodes. Journal of Alloys and Compounds, 2019, 803, 664-670.	2.8	27
66	Stabilizing the structure of LiMn <sub>0.5</sub> Fe <sub>0.5</sub> PO <sub>4</sub> <i>via</i> the formation of concentration-gradient hollow spheres with Fe-rich surfaces. Nanoscale, 2019, 11, 3933-3944.	2.8	27
67	Highly conductive graphene-modified TiO2 hierarchical film electrode for flexible Li-ion battery anode. Electrochimica Acta, 2019, 313, 10-19.	2.6	27
68	Purifying the Phase of NaTi <sub>2</sub> (PO <sub>4</sub> ) <sub>3</sub> for Enhanced Na <sup>+</sup> Storage Properties. ACS Applied Materials & Interfaces, 2019, 11, 10663-10671.	4.0	27
69	A V2O3@N–C cathode material for aqueous zinc-ion batteries with boosted zinc-ion storage performance. Rare Metals, 2022, 41, 1605-1615.	3.6	26
70	Graphene foam supported multilevel network-like NiCo2S4 nanoarchitectures for robust lithium storage and efficient ORR catalysis. New Journal of Chemistry, 2017, 41, 115-125.	1.4	25
71	A three-dimensional cathode matrix with bi-confinement effect of polysulfide for lithium-sulfur battery. Applied Surface Science, 2018, 427, 396-404.	3.1	23
72	LiAlCl4·3SO2 as a high conductive, non-flammable and inorganic non-aqueous liquid electrolyte for lithium ion batteries. Electrochimica Acta, 2018, 286, 77-85.	2.6	23

#	Article	IF	CITATIONS
73	Metal–organic framework derived 3D graphene decorated NaTi <sub>2</sub> (PO <sub>4</sub> ) <sub>3</sub> for fast Na-ion storage. Nanoscale, 2019, 11, 7347-7357.	2.8	23
74	Controllable synthesis of micro/nano-structured MnCo <sub>2</sub> O <sub>4</sub> with multiporous core–shell architectures as high-performance anode materials for lithium-ion batteries. New Journal of Chemistry, 2015, 39, 8416-8423.	1.4	21
75	Seamless alloying stabilizes solid-electrolyte interphase for highly reversible lithium metal anode. Cell Reports Physical Science, 2022, 3, 100785.	2.8	21
76	Mesoporous Ni Co based nanowire arrays supported on three-dimensional N-doped carbon foams as non-noble catalysts for efficient oxygen reduction reaction. Microporous and Mesoporous Materials, 2016, 231, 128-137.	2.2	20
77	Electrochemical performance of Bi 2 O 2 CO 3 nanosheets as negative electrode material for supercapacitors. Ceramics International, 2017, 43, 9310-9316.	2.3	20
78	Graphene-immobilized flower-like Ni3S2 nanoflakes as a stable binder-free anode material for sodium-ion batteries. International Journal of Minerals, Metallurgy and Materials, 2018, 25, 88-93.	2.4	20
79	Mo <sub>2</sub> C-embedded biomass-derived honeycomb-like nitrogen-doped carbon nanosheet/graphene aerogel films for highly efficient electrocatalytic hydrogen evolution. New Journal of Chemistry, 2020, 44, 1147-1156.	1.4	20
80	One-step synthesis of the nickel foam supported network-like ZnO nanoarchitectures assembled with ultrathin mesoporous nanosheets with improved lithium storage performance. RSC Advances, 2015, 5, 81341-81347.	1.7	18
81	A rational VO2 nanotube/graphene binary sulfur host for superior lithium-sulfur batteries. Journal of Alloys and Compounds, 2020, 838, 155504.	2.8	18
82	Three-dimensional nitrogen-doped graphene aerogel toward dendrite-free lithium-metal anode. Ionics, 2020, 26, 13-22.	1.2	17
83	A study on LiFePO <sub>4</sub> /graphite cells with built-in Li <sub>4</sub> Ti <sub>5</sub> O <sub>12</sub> reference electrodes. RSC Advances, 2018, 8, 18597-18603.	1.7	15
84	Superior methanol electrooxidation activity and CO tolerance of mesoporous helical nanospindle-like CeO <sub>2</sub> modified Pt/C. RSC Advances, 2015, 5, 64261-64267.	1.7	12
85	Stress-release design for high-capacity and long-time lifespan aqueous zinc-ion batteries. Materials Today Energy, 2021, 21, 100799.	2.5	12
86	Construction of air-stable pre-lithiated SiOx anodes for next-generation high-energy-density lithium-ion batteries. Cell Reports Physical Science, 2022, 3, 100872.	2.8	12
87	Red phosphorus encapsulated in porous carbon derived from cigarette filter solid waste as a promising anode material for lithium-ion batteries. Ionics, 2018, 24, 3393-3403.	1.2	11
88	Characteristics of Welding and Arc Pressure in the Plasma–TIG Coupled Arc Welding Process. Metals, 2018, 8, 512.	1.0	11
89	Soft-templated synthesis of core–shell heterostructured Ni <sub>3</sub> S <sub>2</sub> @polypyrrole nanotube aerogels as anode materials for high-performance lithium ion batteries. New Journal of Chemistry, 2021, 45, 13127-13136.	1.4	11
90	A LiFePO <sub>4</sub> /Li <sub>2</sub> S <sub>n</sub> hybrid system with enhanced Li-ion storage performance. New Journal of Chemistry, 2018, 42, 6626-6630.	1.4	9

#	Article	IF	CITATIONS
91	Interface coupling in FeOOH/MXene heterojunction for highly reversible lithium-ion storage. Materials Today Energy, 2021, 19, 100584.	2.5	9
92	Li <sub>3</sub> V <sub>2</sub> (PO <sub>4</sub> ) <sub>3</sub> as a cathode additive for the over-discharge protection of lithium ion batteries. RSC Advances, 2016, 6, 76933-76937.	1.7	8
93	Bioinspired hierarchical cross-linked graphene–silicon nanofilms <i>via</i> synergistic interfacial interactions as integrated negative electrodes for high-performance lithium storage. Physical Chemistry Chemical Physics, 2020, 22, 2105-2114.	1.3	8
94	Characterization and Expression Pattern Analysis of the T-Complex Protein-1 Zeta Subunit in Musca domestica L (Diptera). Journal of Insect Science, 2017, 17, .	0.6	7
95	LiAlCl4·3SO2: a promising inorganic electrolyte for stable Li metal anode at room and low temperature. Ionics, 2019, 25, 4137-4147.	1.2	7
96	Long-term cycling stability of NiCo <sub>2</sub> S <sub>4</sub> hollow nanowires supported on biomass-derived ultrathin N-doped carbon 3D networks as an anode for lithium-ion batteries. Chemical Communications, 2021, 57, 1002-1005.	2.2	7
97	Hot-assisted Ultrasonic Additive Manufacturing Method for Al/Cu Layer-metal Composites. Jixie Gongcheng Xuebao/Chinese Journal of Mechanical Engineering, 2018, 54, 95.	0.7	7
98	Lithium fluoride additive for inorganic LiAlCl4·3SO2 electrolyte toward stable lithium metal anode. Electrochimica Acta, 2020, 345, 136193.	2.6	6
99	A stable protective layer toward high-performance lithium metal battery. Ionics, 2019, 25, 4067-4074.	1.2	5
100	Construction of Dualâ€Carbon Coâ€Modified LiFePO 4 Nanocrystals via Microreactor Strategy for Highâ€Performance Lithium Ion Batteries. Energy Technology, 2020, 8, 2000171.	1.8	5
101	An ultrahigh pressure homogenization technique for easily exfoliating few-layer phosphorene from bulk black phosphorus. Physica B: Condensed Matter, 2018, 537, 18-22.	1.3	4
102	Precast solid electrolyte interface film on Li metal anode toward longer cycling life. Ionics, 2020, 26, 1711-1719.	1.2	4
103	Biomolecule-assisted synthesis of porous network-like Ni <sub>3</sub> S <sub>2</sub> nanoarchitectures assembled with ultrathin nanosheets as integrated negative electrodes for high-performance lithium storage. New Journal of Chemistry, 2020, 44, 14453-14462.	1.4	4
104	Grapheneâ€Modified Mesoporous Iron Phosphate as Superior Binary Sulfur Host for Lithium–Sulfur Batteries. Energy Technology, 2020, 8, 1901462.	1.8	4
105	Preparation and controllable prelithiation of core–shell SnO <sub><i>x</i></sub> @C composites for high-performance lithium-ion batteries. CrystEngComm, 2022, 24, 3189-3198.	1.3	4
106	A LiA1Cl4·3SO2-NaAlCl4·2SO2 binary inorganic electrolyte with improved electrochemical performance for Li-metal batteries. Ionics, 2019, 25, 4751-4760.	1.2	3
107	Optically active multi-helical erythrocyte-like Ln(OH)CO <sub>3</sub> (Ln = La, Ce, Pr and Sm). Physical Chemistry Chemical Physics, 2016, 18, 20261-20265.	1.3	2
108	3D Alkâ€MXene@Fe 3 O 4 as Cathode Additive for Rechargeable Lithiumâ^'Sulfur Batteries. Advanced Energy and Sustainability Research, 0, , 2100167.	2.8	1

#	Article	IF	CITATIONS
109	Study on modification and failure of precast solid electrolyte interface film on Li metal anodes. International Journal of Energy Research, 2021, 45, 14034-14046.	2.2	0